Impact of Concrete-Encased Electrodes on Lightning Performance of Grounding Systems

Walter Luiz Manzi de Azevedo
School of Electrical and Computer Eng.
University of Campinas-UNICAMP
Campinas, Brazil
w157573@unicamp.br

José Luciano Aslan D'Annibale
School of Electrical and Computer Eng.
University of Campinas-UNICAMP
Campinas, Brazil
j830494@dac.unicamp.br

Wagner Costa da Silva
School of Electrical and Computer Eng.
University of Campinas-UNICAMP
Campinas, Brazil
w223738@dac.unicamp.br

Anderson Ricardo Justo de Araújo
School of Electrical and Computer Eng.
University of Campinas-UNICAMP
Campinas, Brazil
ajaraujo@unicamp.br

José Pissolato Filho
School of Electrical and Computer Eng.
University of Campinas-UNICAMP
Campinas, Brazil
pisso@unicamp.br

***Abstract*—This paper investigates the influence of concrete-encased grounding earthing system on the harmonic grounding impedance (HGI), and generated Ground Potential Rise (GPR) waveforms. For this purpose, a 3-meter vertical rod embedded in frequency-dependent (FD) soil and encapsulated in concrete is analysed and compared with a bare rod buried in the same soil. The soil is characterized by three distinct values of low-frequency resistivity (ρ_0) of 100, 612 and 1,142 Ω.m. The numerical analysis is performed using the full-wave electromagnetic simulation software *FEKO* (Altair Engineering®), employing the Method of Moments (MoM). First, the harmonic grounding impedance (HGI) of the rod is calculated for frequencies ranging from 100 Hz to 10 MHz. Subsequently, the GPR waveforms generated by impulsive currents are evaluated using two types of injected lightning currents: the first positive impulse (FPI) of 200 kA–10/350 μs and the subsequent negative impulse (SNI) of 50 kA–1/200 μs. The results demonstrate that the concrete-encased rod significantly reduces the harmonic grounding impedance. Moreover, the corresponding GPR waveforms exhibit lower peak values compared to those of the bare rod, indicating that concrete is a promising alternative for mitigating potentials around earthing systems during transient events.**

***Index Terms*—Electromagnetic transient, lightning, grounding systems, soil modelling, low resistivity materials**

I. Introduction

Grounding systems (GS) play a crucial role in power systems during transient events by providing a low-impedance path to divert surge currents into the earth. Based on this requirement, the grounding system must be properly designed to achieve minimal impedance, whose value depends on the geometrical parameters of the GS and the soil properties [1]. When it is not possible to install long rods or electrodes in a given area, soil treatment involving the addition of low-resistivity materials (LRM) can be an effective alternative to reduce the grounding system impedance [1]–[3]. The most commonly used materials include concrete, bentonite, and conductive cement. Regarding concrete, its resistivity is influenced by several factors such as water content, saturation level, composition, temperature, and curing time. According to the literature, the resistivity of concrete varies between 30 and 200 Ω·m [3]. Recently, various studies have investigated the harmonic impedances and/or transient responses of different types of grounding systems, particularly those employing concrete-encased rods or horizontal electrodes in tower-footing grounding configurations [1]–[3]. Different methods have been applied in the literature to evaluate the effect of concrete in grounding systems: (i) field or laboratory measurements [1], [2], and (ii) simulations using full-wave electromagnetic software with numerical methods such as the Finite Element Method (FEM), as reported in [3]–[6]. This paper investigates the influence of concrete encapsulation on grounding rods buried in frequency-dependent (FD) soils, focusing on its impact on GPR waveforms. For this purpose, a 3-meter vertical rod, with and without concrete encapsulation, is analysed for three distinct values of soil resistivity-100, 612 and 1142 Ω.m. The harmonic impedance of the rod is evaluated using the full-wave electromagnetic simulation software *FEKO* (Altair Engineering®), employing the Method of Moments (MoM) for a large frequency range. The Ground Potential Rise (GPR) waveforms are generated using two types of lightning currents: the first positive impulse (FPI) of 200 kA–10/350 μs and the subsequent negative impulse (SNI) of 50 kA–1/200 μs. The results show that the presence of concrete surrounding the rods significantly reduces the harmonic grounding impedance over the frequency range. As a consequence, the GPR waveforms

This work was funded by the Coordenação de Aperfeiçoamento de Pessoal de Nível Superior (CAPES)-Finance code 001 and by São Paulo Research Foundation (FAPESP) grant numbers: 2019/01396-1 and 2021/11258-5.

979-8-3315-8138-1

generated with concrete-encased rods exhibit considerably lower peak values compared to those obtained with bare rods. The contribution of this paper is to assess the impact of concrete on the transient response of grounding rods and to demonstrate that concrete is an interesting alternative to provide safety in earthing system during transient events.

II. Electromagnetic Modelling

A. Soil Modelling

The soil electrical parameters resistivity (ρ_s) and relative permittivity (ε_{rg}) are dependent on frequency due to the polarization mechanisms in the soil particles [7]. Based on Alipio and Visacro model, detailed in [7], CIGRÈ Working Group recommends the following expressions for the FD resistivity and relative permittivity [8]:

$$\rho_s(f) = \rho_0 \left\{1 + 4.7 \times 10^{-6} f^{0.54} \rho_0^{0.73}\right\}^{-1}, \tag{1}$$

$$\varepsilon_r(f) = 12 + 9.5 \times 10^4 \rho_0^{-0.27} f^{-0.46}, \tag{2}$$

where ρ_0 (Ω.m) is the low-frequency resistivity measured at 100 Hz, f (Hz) is the frequency.

B. Low-frequency resistance of horizontal electrode

The low-frequency resistance of the coated electrode can be calculated using the expression [9]

$$R_{LF} = R(\ell, r_0, \rho_c) - R(\ell, r_c, \rho_c) + R(\ell, r_c, \rho_s) \tag{3}$$

where ρ_c is the resistivity of the concrete, ρ_s is the soil resistivity; r_0 is radius of the bare metallic conductor, r_c is the radius of concrete, and ℓ is the conductor length; Each term of the (3) are given as follows:

- $R(\ell, r_0, \rho_c)$: resistance of an electrode with a radius r_0, buried in a soil of resistivity ρ_c;
- $R(\ell, r_c, \rho_c)$: resistance of an electrode with a radius of r_c, buried in a soil of resistivity ρ_c;
- $R(\ell, r_c, \rho_s)$: resistance of an electrode with radius of r_c, buried in a soil of resistivity ρ_s;

The resistance of vertical (v) and horizontal (h) conductor buried in a homogeneous soil is given by [3], [9]:

$$R_v(\ell, r^*, \rho^*) = \frac{\rho^*}{2\pi\ell} \ln\left[\left(\frac{4\ell}{r^*}\right) - 1\right] \tag{4}$$

$$R_h(\ell, r^*, \rho^*) = \frac{\rho^*}{\pi\ell} \ln\left[\left(\frac{2\ell}{\sqrt{2r^* h}}\right) - 1\right] \tag{5}$$

where the variables with (*) are those presented previously and replace accordingly to each term. To assess the harmonic grounding impedance (HGI) of the earthing system (bare conductor or embedded in concrete), the full-wave electromagnetic software FEKO, using numerical Method of Moments (MoM) is employed, as detailed in [10].

TABLE I: Parameters of Heidler function

Parameter	Heidler	
	FPI	SNI
I_0 [kA]	200	50
η	0.930	0.993
n	10	10
τ_1 [μs]	19	0.454
τ_2 [μs]	485	143

C. Lightning Current and Grounding Potential Rise

The lightning strike is represented by an impulsive current source which can be expressed by the Heidler's function given by [11]

$$i(t) = \frac{I_0}{\eta} \frac{(t/\tau_1)^n}{1 + (t/\tau_1)^n} e^{-t/\tau_2}, \tag{6}$$

$$\eta = \exp\left[-\left(\frac{\tau_1}{\tau_2}\right)\left(n\frac{\tau_2}{\tau_1}\right)\right]^{1/n}, \tag{7}$$

where I_0 [A] is the peak current, τ_1 is the time constant for the front of the current wave, τ_2 [s] is the time constant for the tail of the current wave, and t is the time. The n and η are the constant for the steepness and peak correction factors,respectively. TThe values of the lightning current parameters are presented in Table I, while the corresponding lightning current waveforms are illustrated in Fig. 1. In Fig. 1(a), the SNI waveform exhibits a significantly shorter front time compared to the FPI, although its peak amplitude is approximately one-quarter that of the FPI. Furthermore, the SNI shows a higher current derivative, as expected, due to its steeper front time in the initial stage of the waveform. Consequently, the frequency spectrum of the SNI is considerably broader than that of the FPI, as illustrated in Fig. 1(b). The GPR can be calculated in time domain by [12]:

$$v(t) = \mathscr{F}^{-1}\left\{Z_{\text{fit}}(j\omega) \times I(j\omega)\right\} \tag{8}$$

where $\mathscr{F}$ represents the Fourier transform which can be solved by using a numerical recursive convolution method [12].

III. Numerical results and discussions

A. Low-frequency resistance

To quantify the impact of different radii of encapsulating concrete on the earthing conductor, simulations with both vertical and horizontal electrodes are performed in this section. For this purpose, the length ℓ of each conductor is set to 10 m, the conductor radius r to 7 mm, and the burial depth h to 0.5 m. The concrete resistivity ρ_c is assumed to be 30 Ω·m, based on [3], while the soil resistivity ρ_s varies from 100 to 1,000 Ω·m. Distinct concrete radii r_c of 5, 10, 20, and 30 cm are considered. The resistances are calculated using (3) to (5). The simulated resistance values for both conductors are illustrated in Fig. 2. As shown in the figure, the resistance of both conductors decreases with increasing radius of the encapsulating concrete, reaching its minimum value at r_c = 30 cm. The corresponding percentage difference (Δ) for the soil with a resistivity of 1,000 Ω · m is also presented, confirming that the greatest variation occurs at r_c = 30 cm.

979-8-3315-8138-1

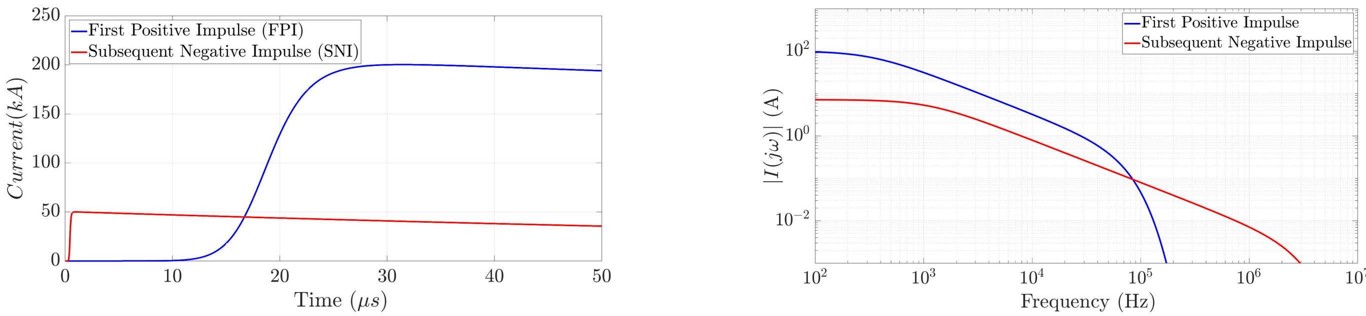

(a) (b)

Fig. 1: (a) Lightning current waveforms for the FPI and SNI; (b) Fourier magnitude of the lightning currents.

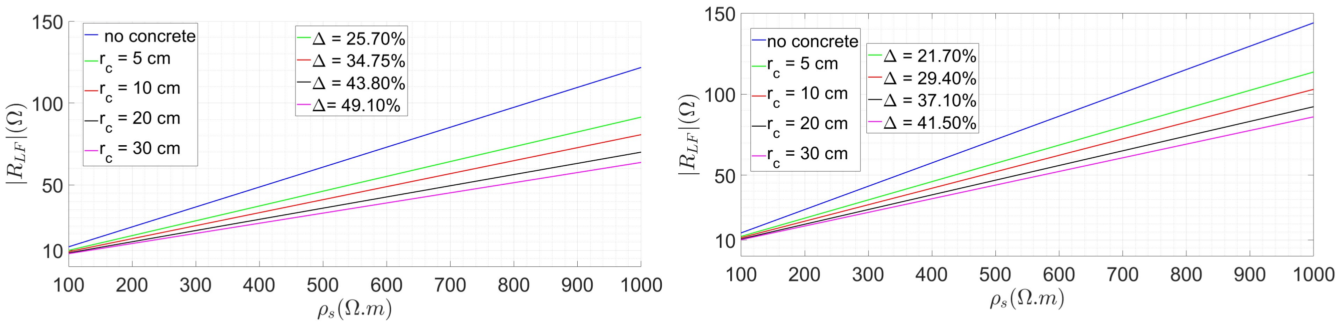

(a) (b)

Fig. 2: Resistance for different radii of encapsulating concrete: (a) 10-m vertical rod; (b) 10-m horizontal electrode.

B. Validation of coated earthing system

To validate the simulation model of the metallic conductor coated with a material (concrete), the numerical results are compared with those obtained by Bezerra *et al.* in [3] for a 10-m horizontal electrode, buried at a depth of 0.5 m in soil with a resistivity of 300 $\Omega \cdot$ m, relative permittivity ε_r = 10, and coated with a concrete characterized by low-frequency resistivity of 30 $\Omega \cdot$ m, and a diameter of 20 cm. The harmonic grounding impedance (HGI) is evaluated over a frequency range from 100 Hz to 4 MHz, taking into account the frequency dependence of soil parameters as per the CIGRE WG recommendations [8]. The calculated HGI magnitude and phase are plotted in Figs. 3(a) and (b). As observed, a good agreement is obtained at low frequencies up to 100 kHz. Above this frequency, the HGI calculated by FEKO becomes more pronounced and starts to deviate from those assessed by Bezerra *et al.* in [3]. The developed GPR for the lightning current of FPI ans SNI are shown in Figs 3(c) and (d), respectively.According to the figures, acceptable agreement is observed over the entire time range, with percentage differences (Δ) at peak values of 4.23% and 14.08% for the FPI and SNI, respectively.

C. Harmonic Grounding Impedance

To investigate the influence of the concrete-encased rods buried in a FD soil on the GPR waveforms, the HGI of the vertical rod buried in a homogeneous ground is computed for three values of low-frequency resistivity (ρ_0): 100, 612, and 1,142 Ω.m. The FD resistivity and permittivity are calculated using (1) and (2). The simulation results are compared with those generated with bare rod buried at the same soils. The length of rod ($\boldsymbol{\ell}$) is 3 m, radius of r = 12.5 mm and the concrete radius of r_c = 10 cm, concrete resistivity ρ_c of 30 Ω.m were considered. The harmonic grounding impedance (HGI) is calculated for frequencies ranging from 100 Hz to 10 MHz, as shown in Fig. 4. According to this figure, it can be observed that both the soil parameters have a significant influence on the HGI across the analysed frequency range. At lower frequencies (below 1 kHz), the HGI exhibits a predominantly resistive behaviour for both types of rods, up to a certain transition frequency. This resistance is proportional to the low-frequency resistivity ρ_0 for the bare rod and to the equivalent resistivity for the concrete-encased rod, as illustrated in Fig. 4. However, as the frequency increases, the reactive behaviour of the harmonic impedance becomes more pronounced, alternating between inductive and capacitive characteristics depending on the frequency range and the equivalent soil resistivity. Furthermore, regarding the magnitude of the HGI, the concrete-encased rod (represented by the dashed line) exhibits lower values compared to those of the bare rod (represented by the solid line) across the entire frequency range. This reduction is attributed to the lower

979-8-3315-8138-1

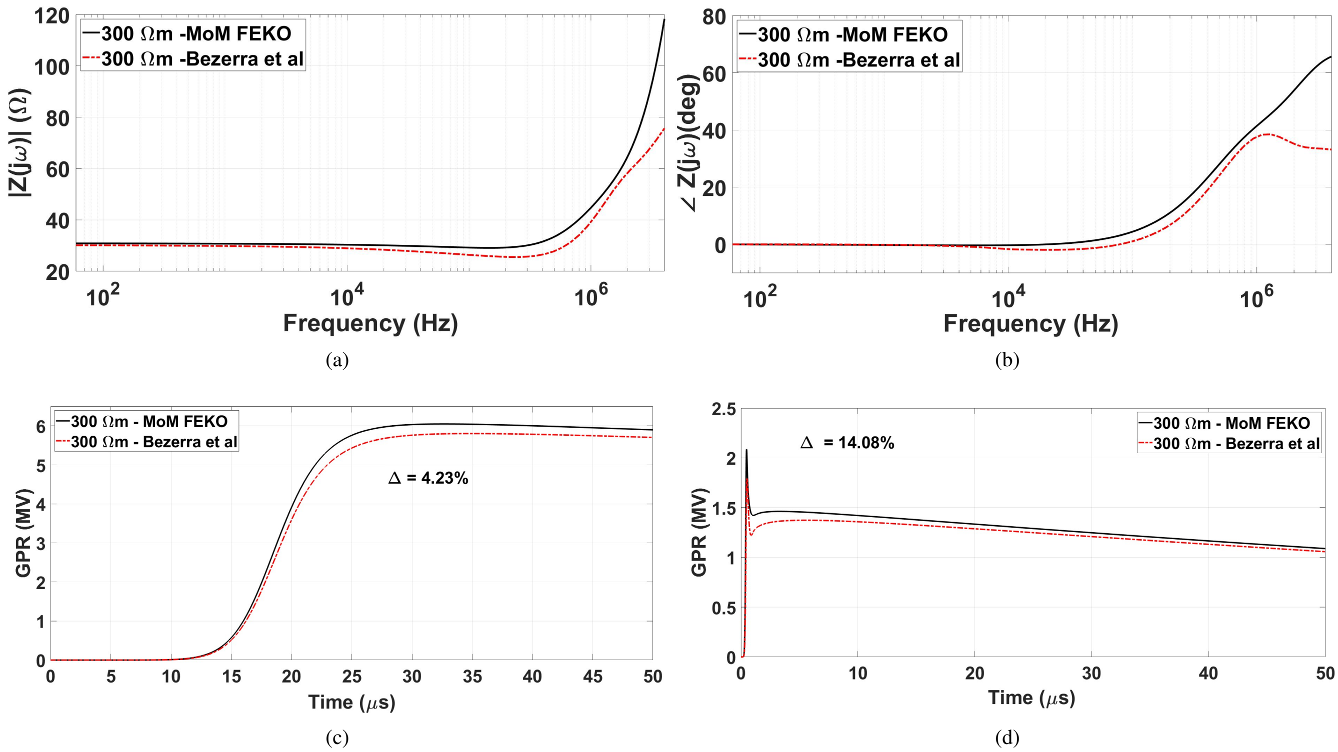

Fig. 3: Validation using FEKO compared with Bezerra *et al.* in [3]: (a) Magnitude; (b) Phase; GPR developed for: (c) FPI; (d) SNI.

equivalent resistance obtained when concrete is added around the metallic rod, interpreted as a new conductor of radius r_c.

D. Transient Ground Potential Rise

The generated Ground Potential Rise (GPR) is computed in the time domain, considering lightning current waveforms representative of the first positive impulse (FPI) of 200 kA–10/350 μs and the subsequent negative impulse (SNI) of 50 kA–1/200 μs. The transient GPR waveforms for both types of rods are presented in Fig. 5, and their corresponding peak values (with percentage reductions) are listed in Table II. According to the table, the use of concrete around the rod results in a reduction of approximately 42% in the peak GPR values. In general, the transient GPR waveforms are strongly dependent on the lightning current waveform and the electrical parameters of the soil. The peak GPR values increase with increasing soil resistivity for both types of lightning impulses. However, a notable reduction in the peak values is observed for the concrete-encased rod compared to those of the bare rod. For the GPR generated by the subsequent negative impulse (SNI), as shown in Fig. 5(b), the peak magnitudes are lower than those produced by the first positive impulse (FPI). This reduction is attributed to the lower equivalent resistivity introduced by the concrete surrounding the metallic rod, compared with the bare-rod configuration.

The numerical results demonstrate that concrete-encased rods significantly reduce the low-frequency resistance, harmonic impedance, and consequently the potential rise when used as an encapsulating material in earthing systems, thereby enhancing their overall effectiveness. In addition to improving electrical performance, concrete provides corrosion protection, which is essential for maintaining reliable and safe grounding performance over time. Moreover, concrete offers a combination of mechanical strength and durability to the tower base, while its ability to retain moisture and release ions from certain chemical additives improves the conductivity of the surrounding soil.

TABLE II: Peak values of GPR(MV) and percentage difference (%)

ρ_s [Ω m]	Bare		Encased		Difference	
	FPI	SNI	FPI	SNI	FPI	SNI
100	7.15	1.73	4.17	1.01	41.69%	41.68%
621	42.5	9.88	24.8	5.76	41.68%	41.68%
1142	75.8	17.3	44.2	10.1	41.69%	41.69%

IV. Conclusions

This paper investigates the influence of concrete on the harmonic grounding impedance (HGI) and the resulting Ground Potential Rise (GPR) waveforms for bare and concrete-encased rods buried in frequency-dependent soils. A 3-meter vertical rod is analysed in soils with different low-frequency resistivity values, and the harmonic grounding impedance is computed using full-wave electromagnetic simulation software over a frequency range from 100 Hz to 10 MHz. The results indicate that the HGI is predominantly resistive at low frequencies but becomes increasingly reactive at higher frequencies. In

979-8-3315-8138-1

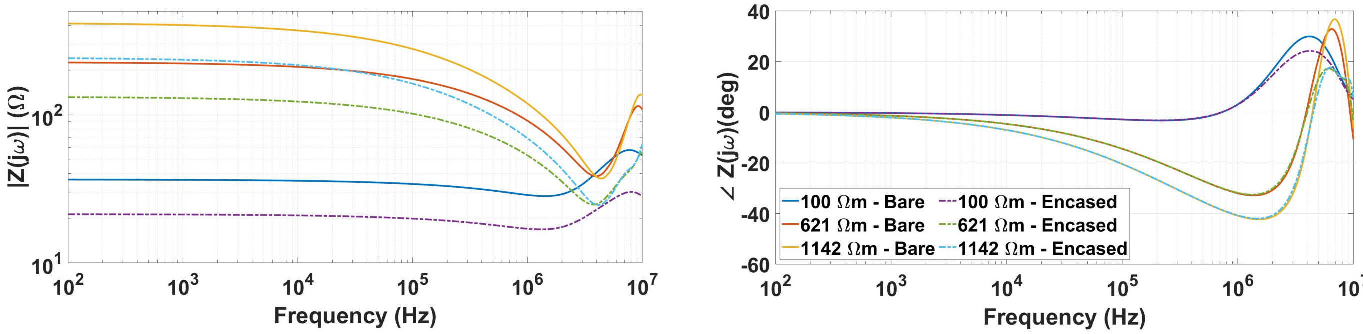

(a) (b)

Fig. 4: Harmonic grounding impedance of the bare and concrete encased 3-m rods: (a) Magnitude; (b) Phase.

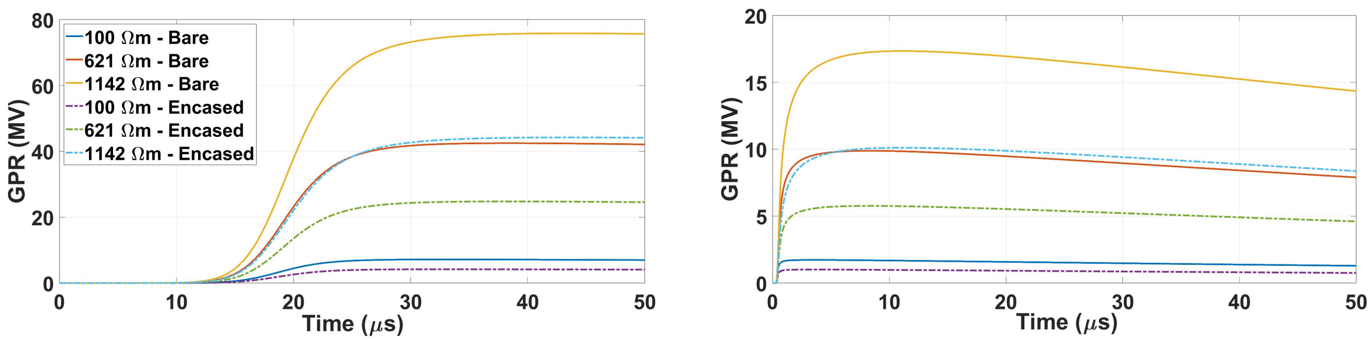

(a) (b)

Fig. 5: Transient GPR generated for the bare and concrete encased 3-m rods for: (a) FPI (b) SNI

general, the HGI obtained for concrete-encased rods is considerably lower than that of bare rods, owing to the reduced apparent soil resistivity and the increased effective radius introduced by the surrounding concrete layer. Regarding the transient GPR waveforms, the peak values are significantly reduced when concrete is employed, demonstrating improved lightning performance for concrete-encased rods compared with conventional bare rods. These findings emphasize the substantial impact of concrete on the lightning transient behaviour and overall performance of grounding systems under impulsive conditions.

References

[1] O. Kherif, S. Robson, H. Griffiths, N. Harid, D. Thorpe, and A. Haddad, “On the high frequency performance of vertical ground electrodes and lrm application,” *IEEE Transactions on Electromagnetic Compatibility*, 2024.

[2] A. Raizer, E. P. Elias, M. V. F. da Luz, V. L. Coelho, V. M. Raupp, M. Telló, and J. M. Giannini Júnior, “Traditional and alternative grounding system’s impedance and resistance measurements of a 138 kv transmission line tower,” *Electric Power Systems Research*, vol. 231, p. 110358, 2024.

[3] G. V. N. Bezerra, F. A. Moreira, T. V. Ferreira, and R. Alipio, “Concrete encased grounding: Lightning response analysis considering the frequency dependence of soil,” *IEEE Transactions on Electromagnetic Compatibility*, vol. 66, no. 3, pp. 879–889, 2024.

[4] N. A. S. Hasni, S. N. M. Arshad, A. M. Ariffen, N. H. Halim, W. C. Leong, M. I. F. Romli, and O. A. Bakar, “Effect of concrete orientation as an enhancement material in grounding system,” in *IOP Conference Series: Materials Science and Engineering*, vol. 864, no. 1. IOP Publishing, 2020, p. 012163.

[5] M. Daadaa, S. Brettschneider, C. Volat, and G. Simard, “Numerical investigation of the use of electrically conductive concrete-encased electrodes as potential replacement for substation grounding systems,” *Energies*, vol. 16, no. 11, 2023.

[6] M. Talaat, M. Farahat, M. A. Essa, and M. Maowwad, “Simulation of the electric field and the gpr resulting from vertical-driven rods earthing system in a multi-layers earth structure,” *Measurement*, vol. 132, pp. 387–401, 2019.

[7] R. Alipio and S. Visacro, “Modeling the frequency dependence of electrical parameters of soil,” *IEEE Transactions on Electromagnetic Compatibility*, vol. 56, no. 5, pp. 1163–1171, 2014.

[8] CIGRE-WG4.33, “Impact of soil-parameter frequency dependence on the response of grounding electrodes and on the lightning performance of electrical systems,” *Technical Brochure 781*, 2019.

[9] G. Bezerra, “Avaliação da resposta transitória de aterramentos encapsulados por concreto,” Ph.D. dissertation, 11 2024.

[10] FEKO, “FEKO Altair Engineering,,” 2023. [Online]. Available: www.hyperworks.com/feko.

[11] B. R. Terespolsky, H. G. P. Hunt, and K. J. Nixon, “An approximation to the heidler function with an analytical integral,” *IEEE Transactions on Electromagnetic Compatibility*, vol. 66, no. 4, pp. 1153–1167, 2024.

[12] J. Colqui, A. de Araújo, C. M. de Seixas, S. Kurokawa, and J. Pissolato Filho, “Performance of the recursive methods applied to compute the transient responses on grounding systems,” *Electric Power Systems Research*, vol. 196, p. 107281, 2021.